Journal section: Behavioral Neuroscience

Chemogenetic inhibition of a cortical motor area impairs vocal control in singing zebra finches.

Yoko Yazaki-Sugiyama,[1] Shin Yanagihara,[1] Patrick M Fuller,[2] and Michael Lazarus[3]

[1]Neuronal Mechanism for Critical Period Unit, Okinawa Institute of Science and Technology (OIST) Graduate University; [2]Division of Sleep Medicine, Harvard University; [3]International Institute for Integrative Sleep Medicine (WPI-IIIS), University of Tsukuba

Corresponding author:

Yoko Yazaki-Sugiyama: yazaki-sugiyama@oist.jp

Neuronal Mechanism for Critical Period Unit, OIST Graduate University, 1919-1, Tancha, Onna-son, Okinawa, 904-0495, Japan

FAX: +81-98-966-2891

Running title: A subset of neurons controls a specific song part.

Total number of pages: 34 pages (incl. this page)

Total number of figures: 11 figures

Total number of tables: no table

Total number of equations: no equation

Total number of words: Whole manuscript: 6791 words

Abstract: 191 words

Introduction: 541 words

Keywords: Motor pattern generation, pharmacogenetic tools, singing behavior, song motif

Abstract

Genetically-targeted approaches that permit acute and reversible manipulation of neuronal circuit activity have enabled an unprecedented understanding of how discrete neuronal circuits control animal behavior. Zebra finch singing behavior has emerged as an excellent model for studying neuronal circuit mechanisms underlying the generation and learning of behavioral motor sequences. We employed a newly developed, reversible, neuronal silencing system in zebra finches to test the hypothesis that ensembles of neurons in the robust nucleus of the arcopallium (RA) control the acoustical structure of specific song parts, but not the timing, nor the order of song elements. Subunits of an Ivermectin (IVM)-gated chloride channel were expressed in a subset of RA neurons, and ligand administration consistently suppressed neuronal excitability. Suppression of activity in a group of RA neurons caused the birds to sing songs with degraded elements, although the order of song elements was unaffected. Furthermore some syllables disappeared in the middle or at the end of song motifs. Thus, our data suggest that generation of specific song parts is controlled by a subset of RA neurons, whereas elements order coordination and timing of whole songs are controlled by a higher premotor area.

Introduction

As in human speech, vocalization is recognized and generated as a sequence of motor patterns. To generate and recognize specific patterned vocalizations, well-coordinated neuronal circuits are required. Bird songs serve as the premier model for studying central motor circuits subserving song motor pattern generation and learning. The zebra finch is the most commonly used model by virtue of its stereotyped song patterns and well-described brain anatomy. Zebra finch songs generally consist of a few acoustical elements, called syllables, which emerge in a stereotyped sequence. In zebra finches, brain areas subserving song production and learning, i.e. the "song system," are well identified. The premotor area, HVC (used as a proper name) sits at the apex of the song system, and in turn, projects to a secondary premotor region, called the robust nucleus of the arcopallium (RA) (Nottebohm et al., 1982, Wild, 1993). The RA comprises of thousands of neurons, each of which topographically projects to subregions of the hypoglossal motor nucleus, which in turn directly innervates the vocal organ syrinx, or dorsomedial (DM) nucleus of the midbrain intercollicular complex (ICo) (Gurney, 1981; Vicario, 1991; Vicario & Nottebohm 1993). The temporal organization of zebra finch song pattern generation is linked to sparse spike firing by HVC neurons (Harhnloser et al., 2002), which have been suggested to produce bursts in RA neurons at different points in song motifs (Fee et al., 2004; Leonardo & Fee, 2005). RA neurons show high-frequency bursts that are precisely reproduced during song

motif repetition (Yu and Margoliash, 1996; Chi and Margoliash, 2001; Leonardo and Fee, 2005), and their pattern is depending on notes (subsyllable) type, suggesting that the activity of RA neurons controls acoustical structure of syllables. These observations further suggest that RA neuronal stereotyped firing is necessary for stereotype of bird song.

Many of previous studies employing neurotoxic lesioning (Ashmore et al., 2008), electrophysiological recordings (McCasland & Konishi, 1981; Mooney, 2000; Fee & Leonardo, 2001; Long & Fee, 2010 and others), or pharmacological approaches (Olveczky et al, 2005; Charlesworth et al, 2012) have revealed the neuronal circuit mechanism for zebra finch singing behavior, i.e., the stereotyped motor outputs. Given the recent development of genetically-targeted systems that enable acute and reversible activation or inactivation of discrete neuronal circuit elements, we tested the hypothesis of previous studies that ensembles of RA neurons control acoustical structure of song elements. Although the lack of efficient transgenic zebra finches has hampered the use of genetic tools in this model system (Agate et al., 2009), viral vector gene delivery systems (Roberts et al., 2012) could theoretically enable development of a zebra finch model system for studying the detailed circuit basis of motor pattern generation and learning. To generate such a model, we used adeno-associated viral (AAV; serotype 9) vectors to deliver 2 subunits (α and β) of *C. elegans* glutamate- and Ivermectin (IVM)-gated chloride channels (GluCl; Slimko et al., 2002) to RA neurons in zebra finch brains. This allowed us to examine the effects of

reversible silencing of these neurons on song motor generation (Lerchner, 2007) and more specifically on acoustical structures of each song element. Here we show that ensembles of RA neurons contribute to the acoustic structure of specific song parts, but not to the timing or syllable sequence of the songs.

Materials and Methods

All experimental procedures were performed with the approval of the Animal Care Committee at Okinawa Institute of Science and Technology (OIST) Graduate University and in accordance with NIH guidelines for the care and use of animals. Every effort was made to minimize the number of animals used, as well as pain and discomfort.

AAV Production

AAVs of serotype 9 for AAV-optGluClα-EYFP-pACP (AAV-GluClα) and AAV-optGluClβY182F-ECFP-pACP (AAV-GluClβ) (Li et al., 2002; Slimko and Lester, 2003) were generated by tripartite transfection (AAV-rep2/cap9 expression plasmid, adenovirus helper plasmid, and AAV-vector plasmid) into 293A cells. Then the virus titer was determined with qPCR (AAV-GluClα: 4.2×10^{12} and AAV-GluClβ: 3.1×10^{12}). (YFP and CFP denote yellow fluorescent protein and cyan fluorescent protein, respectively.)

Zebra finches

Adult male zebra finches were purchased from commercial sources and maintained in the laboratory. To express GluCl channel subunits, we injected a mixture of AAV-GluClα and AAV-GluClβ into both sides of RAs (1µl over 10-15min) using glass pipettes connected to a pressure injector (Narishige, IM300) with stereotaxic coordination under Equithesin athesthesia (30µl/body). IVM (TOCRIS) solution in propylene glycol or vehicle solution was injected i.p. (1.25 mg/kg BW) before and after AAVs injection. During this process, zebra finches were housed in individual sound attenuation chambers and their songs were recorded (Avisoft) and analyzed later.

Electrophysiology *in vitro*

Sagittal brain slices (400-µm thickness) were made from zebra finches that had been injected more than 2 weeks previously with a mixture of AAV-GluClα and AAV-GluClβ. Throughout experiments, slices were continually perfused with ACSF. Whole–cell patch clamp recordings were made from RA neurons with electrodes having a resistance of 5–8 MU, when filled with pipette solution of the following composition: 135 mM potassium gluconate, 5 mM EGTA, 0.5 mM $CaCl_2$, 2 mM $MgCl_2$, 10 mM HEPES, 2 mM Mg-ATP, and 0.1 mM GTP. Voltage clamp recordings were performed to monitor spontaneous activity and changes in activity following application of IVM (TOCRIS, 20 nM in 1% DMSO/ACSF)

in the bath. To examine the effect of IVM application, we monitored spiking events in five 25-sec recordings taken at each of four time periods: before, during, 15 min after, and 25 min after drug application. After recording, neurons in 50-μm frozen sections were visualized with Alexa647 injected through the recording electrode, and examined for the expression of YFP and CFP.

Electrophysiology *in vivo*

Zebra finches that were injected with AAV-GluClα and AAV-GluClβ and were subjected to electrophysiological recording under isofluorane (1.3%) anesthesia. Extracellular single unit activity was recorded from RAs by stereotaxic cordination using a tetrode. Spontaneous neuronal activity was recorded before, during and after systemic IVM injection (1.25mg/kg). Single units were isolated by post hoc analysis (Plexon).

Song analysis

To see whether birds sang stable songs, we measured song similarity between each bird's songs at different time points and the typical template songs. We created typical syllable templates using the bird's own songs, sung more than 24 hrs before each IVM injection, before and after AAV injections, and performed template matching of songs (a total of 30 song motifs) each day, and then calculated the percentage of syllables that matched the

typical syllable template (coefficient efficiency >0.5) as a similarity index. The typical syllable template constitutes a standard or normal pattern for each bird. We calculated similarity at 10 different time points more than 24 hr before the IVM injection day and used it as the baseline. Then we normalized song similarity before and after IVM injection using the baseline.

Histological analysis.

After the behavioral investigation, birds were transcardially perfused with saline, followed by 4% paraformaldehyde (PFA) and were then post-fixed and cryoprotected overnight with 30% sucrose/PFA. Brains were then sliced into 40-μm sections using a frozen microtome (Leica). Sections were immunohistochemically stained with GFP- (Molecular Probes (Invitrogen), Cat# A6455) and NeuN- (EMD, Millipore, Cat# MAB377) primary antibody, and subsequently stained with a fluorescent secondary antibody (Molecular Probes). Confocal images (Olympus FV-1000) of the RA brain region were captured, and GFP or NeuN-positive cells, as well as YFP- or CFP-expressing cells were counted by an observer who was blind to the birds' treatment histories.

Results

Expression of GluCl channel subunits in zebra finch brain

The feasibility of GluCl/IVM-mediated silencing of neuronal activity *in vivo* has been previously established, but only in mice (Lerchner et al., 2007). We therefore tested whether the GluCl/IVM channel system could be successfully employed in the zebra finch model. We injected a mixture of AAV-GluClα and AAV-GluClβ into RA, and two weeks after the AAV injections, we observed both YFP- and CFP-labelled cells in and around the injection site. Because IVM-dependent inhibition of neuronal activity is only possible in cells that express both the α and β subunits of heteromeric GluCl channels, we quantified co-expression of both subunits by visualizing endogenous YFP and CFP fluorescence using confocal microscopy. We found that 61.4 % of YPF-expressing cells co-expressed CFP and 92.9 % of CFP-expressing cells also expressed YFP (78/127 YFP-labeled cell and 78/84 CFP-labeled cells from 13 sections from 3 birds), demonstrating a high level of subunits co-expression (Figure 1B).

IVM-dependent neuronal silencing *in vitro* and *in vivo*

To confirm the inhibitory effect of IVM on GluCl-expressing neurons in zebra finch brain, we performed whole-cell patch clamp recording from acutely prepared slices. We monitored spontaneous activity of RA neurons in voltage-clamp mode in slices taken from birds that had been injected with the AAV-GluClα/AAV-GluClβ mixture. As we were unable to reliably detect YFP and CFP expression in the 400-μm thick slices used for patch

clamp recording, we instead randomly recorded from the RA area and identified the recorded neuron histologically post-hoc using Alexa647 labeling, which was injected through the recording electrode (Figure 2A). The effect of IVM was determined by monitoring the effect of IVM bath application on the spontaneous activity of RA neurons. RA neurons displayed spontaneous high-frequency firing, which we monitored as action-potential current with voltage clamp recordings (Figure 2B, before). We recorded 8 RA neurons from 7 virus-injected birds with successful post-hoc histological identification. The rate of action potential current was decreased by the bath application of 20 nM IVM in 4 out of the 8 cells that expressed both YFP and CFP (Figure 2C left). In fact, in 3 of 4 YFP/CFP-positive neurons, firing activity was completely absent after IVM applications, and did not recover even 25 min after washing, as previously reported (Lerchner et al, 2007). In the remaining 4 neurons in which we could not detect YFP or CFP fluorescence, the rate of the action-potential current did not change, or occasionally increased after bath application of IVM (Figure 2C, right). Normalized firing rate in neurons that expressed both α and β subunits of GluCl channels was significantly lower when compare to neurons that did not express either subunit during IVM perfusion (normalized firing rate during IVM infusion in YFP/CFP positive neurons vs YFP/CFP negative neurons, 20.2±19.5 vs 129.0±18.4, n=4 and 4, average ±se, $p<0.01$, unpaired t-test). These *in vitro* experiments confirmed

IVM-dependent suppression of neuronal firing in neurons that expressed α and β subunits of GluCl channels.

We next sought to determine if IVM could cross the zebra finch blood-brain barrier, which would enable use of the GluCl/IVM system *in vivo.* To do so, we performed extracellular recordings of spontaneous RA neuronal activity in AAV-GluClα/AAV-GluClβ-injected birds. To maximize the chances of recording from AAV-GluClα/AAV-GluClβ- transduced neurons, we inserted the recording electrode through the same pipet track used for AAV injection. As reported previously (Yu and Margoliash, 1996), RA neurons showed a high rate of (> 10Hz) spontaneous firing, and this firing was significantly suppressed following *i.p.* administration of IVM at 1.25 mg/kg (Figure 3) (Firing rates 10 min before and 20 min after IVM administration were 15.5±2.0 and 3.1± 1.4 Hz, n=5, $p<0.05$, Wilcoxon signed-rank test (one-tailed)). These results suggest that the GluCl/IVM system can be successfully applied to the zebra finch brain *in vivo* to suppress neuronal activity, as has been successfully done in the mouse model (Lerchner et al., 2007).

Effect of suppression of RA neuronal activity on singing behavior

Following validation of the GluCl system in zebra finch brain, we used this system for defining the specific contribution of neurons in the song premotor area RA to zebra finch singing behavior. To elucidate the role of zebra finch RA neuronal activity in motif

generation, we injected AAV-GluClα/AAV-GluClβ into the RA and investigated the effect of silencing RA neurons on singing behavior. Systemic administration of IVM in AAVs uninjected zebra finches (binomial test, $p>0.05$; one bird showed slightly decreased similarity) and expression of GluClα/ GluClβ in the absence of ligand had no effect on the acoustical structure of zebra finch stereotypic song motifs (Figure 4A&B). It has been reported that expression of only a single channel is insufficient to induce behavioral effects (Lechner et al, 2007). Upon IVM administration, however, birds with confirmed GluCl expression in the RA exhibited specific changes in their songs. Five of 7 birds with GluCl expression in the RA changed their songs after IVM injection (decreased song similarity to template songs, Figure 4 B and C, $p < 0.05$ binomial test). In 2 of these 5 birds, songs were degraded when they started to sing again within a few hours after the first IVM injection with AVVs infection, but baseline recovery was observed within 24 hr of the injections. In the remaining 3 birds, singing did not resume until the next morning (~24 hr post-injection), and their singing did not return to normal for up to 8 days. The time-course of IVM-mediated behavioral effect was similar to results reported in mice (Lerchner et al, 2007); the earliest effect was detected 6-12 hr after IVM injection, and maintained in average of 2-3days, with maximum of 14days. Histological analysis revealed a subset of RA neurons (~5% compared to NeuN-labeled cells in RA) in adult male zebra finches that expressed GluCl channels. To maximize the detection of GluCl channel expression, we labeled neurons with

anti-GFP antibody, although it did not allow us to distinguish YFP expression from CFP expression. We counted the number of cells labeled with anti-GFP antibody, as well as the number of neurons labeled with anti-NeuN antibody within the entire RA brain region in both hemispheres. An average of 9.69 % of NeuN labeled RA neurons were also labeled with anti-GFP (9.69±4.05 (Ave±SE), n=7). However one bird had an especially high infection level (33.7%), which affected the average. Without this bird, the average decreased to 5.68± 0.74).

Degradation of songs was also detected as a decrease of identified syllable variety in a motif because birds changed acoustical structures of some syllables (Figure 6 and 7). Furthermore in some birds, the total number of syllables in a motif decreased as they stopped a song in the middle (Figure 8 and 9) or dropped a syllable (Figure 10).

Syllable-specific control by ensembles of RA neurons

An earlier study on unilateral inactivation of the RA using microlesions showed a diminution of almost all parts of a song motif (Ashmore et al., 2008). In the present study, IVM-mediated suppression of RA neuronal activity induced changes only in specific parts of song motifs, essentially on specific syllables. Although the number of affected syllables differed between birds, within a single bird, some syllables showed a decrease in the degree of template matching after IVM injection, whereas other syllables did not (Figure 6~10B).

In any case, IVM application did not change the syllable order, supporting the previously suggested idea that ensembles of RA neurons control the acoustic structure of song elements. Interestingly, songs stopped in the middle of motifs in two birds, and subsequent syllables were not sung (Figure 8 and 9A). In one bird, 1 syllable (#4) was dropped following inactivation of a subset of RA neurons (Figure 10A). This bird's song motif consisted of 6 types of syllables, and we counted 176 syllables in 30 motifs before the IVM injection. However, the number of the identified syllables decreased to 132, representing only 5 types of syllables, 24 hr post-IVM injection. Recovery of the sixth syllable type occurred 3 days post- injection (Figure 10B).

Phasic bursting of RA neurons time-locked to a song motif has been suggested to play an important role in generating stereotype in zebra finch songs. Two motor control models within the forebrain premotor circuit have been suggested and discussed. In one model, a chain of sparse firing of HVC neurons, many of which project onto single RA neurons to drive the precise bursting that produces the song motifs, generates precise timing and control a whole song motif (Fee et al., 2004, Leonardo & Fee, 2005). In another model, time-precise bursting is generated by the interaction of HVC input and RA local circuits, controlling stereotyped song motifs (Yu & Margoliash, 1996; Chi & Margoliash, 2001; Amador et al, 2012). To examine the possibility of temporal pattern control by an upstream area, we further investigated the duration, interval between syllables (beginning of a syllable

to the beginning of the next syllable) and the gap between each pair of syllables (silent period between syllables) before and after IVM injection. In all five birds that changed songs with IVM injections, the duration of syllables or intervals between syllables changed. However, interestingly, elongation or shortening of syllable duration occurred only in some song elements, rather than throughout the entire song, occurred when HVC activity was decreased by cooling (Long & Fee, 2008). The changes in duration of each syllable and the interval were relatively large when compared to the change in the whole motif duration (Figure 11). We compared the duration of the whole motif before and after IVM injection (in birds that stopped songs in the middle of a motif after IVM injection, we compared the duration of the remaining parts). Durations of whole motif were significantly different before and after IVM injection in all five birds. However the amount of difference was small (~5%) and was not equal to the sum of differences in duration and intervals of each syllable. These observations suggest that changes in the duration or interval of each syllable are more affected by changes in acoustic structures, however, precise timing of each syllable could be modified by activity changes of RA local circuits, as suggested by time-precise RA neuronal bursting is thought to be produced in RA local circuits. These data show that silencing of groups of RA neurons had effects on acoustical structures of specific syllables without changing their sequences, supporting the idea that the sequence had already been generated within a neuronal circuit in the upstream premotor area, probably within the microcircuit in

HVC. By contrast, timing of each small song parts and acoustic structure of syllables are controlled by the interaction between HVC inputs to the RA local circuit.

One of the advantages of pharmacogenetic tools is reversible control of neuronal activity and repetitive control of the same circuit. So we injected IVM a second time more than 3 weeks after the first injection. We then confirmed that all 5 birds that showed song degradation with first IVM injection, again sang degraded songs with a second IVM injection (Figure 4B). Before the second injection, song similarity to the template song was recovered to baseline, but again decreased after the second IVM injection to a level comparable to the first injection. These results suggest the presence of firmly formed neuronal circuits susbserving generation of specific syllables within RA.

Discussion

Genetic methods have provided powerful experimental techniques for investigating neuronal mechanisms underlying animal behavior. In particular opto- and pharmacogenetic tools have enabled investigation of links between activities of discrete circuits or cell populations and behavioral and physiological outcomes (Boyden et al., 2005; Li et al., 2005; Nagel et al., 2005). In this study we successfully applied the GluCl/IVM system to reversibly suppress neuronal activity of a subset of RA neurons in behaving zebra finches.

Using this method, we found that ensembles of neurons in the zebra finch forebrain premotor area RA, contribute to generation of specific elements of sequenced motor activities.

Zebra finch singing behavior is a well-characterized learned motor sequence. Brain areas necessary for song production and learning, i.e. the "song system," are well identified. The premotor HVC comprises 3 types of neurons, i.e, projecting neurons for 2 different brain areas and interneurons (Mooney, 2000). Among them, neurons that project to the RA fire sparsely, but are precisely time-locked to specific parts of song motifs during singing (Hahnloser et al., 2002). A model in which RA neurons receive inputs from multiple neurons in the HVC, causing multiple bursting at different points in the song motifs, has been suggested (Fee et al., 2004; Leonardo & Fee, 2005). In this model, temporal coding and song syllable sequences for whole motif are generated within a local circuit in the upstream premotor area, HVC (Long & Fee, 2010). Our results partially support the model that syllable sequence is already coded in HVC. However, inactivating ensembles of RA neurons resulted in changing of acoustic structure as well as local temporal coding of specific syllables. In addition, although the sequence of syllables did not change, some birds dropped syllables in the middle or end of motifs. This suggests that the timing and acoustic structure of syllables are generated within ensembles of RA neurons or RA local circuits with HVC input interaction. This would support the idea of precise RA bursting is controlling each song note. Suppression of just a group of RA neurons resulted in degradation of acoustical

structures only in specific parts of motifs, without changing the other parts, or syllable sequences. Seven syringeal muscles are thought to contribute to song generation (Greenewalt, 1968), and they are innervated by fibers from the hypoglossal motor nucleus. There are about 8000 RA neurons, some of which topographically project to subregions of the hypoglossal motor nucleus (Gurney, 1981; Vicario, 1991). However, the precise connectivity between RA neurons and brainstem motor units is not yet known, and the relationship between syringeal muscle forces and vocal output can be complex (Fee et al., 1998). Some models suggest that just a small number of muscles can directly control acoustical parameters of songs (Gardner et al., 2001; Mindlin et al., 2003). In addition, RA neurons independently project to other parts of the brainstem, the nucleus retroambigualis (Ram) and nucleus parambigualis (PAm), where the neurons are involved in vocal-respiratory coordination (Wild, 1993). In this study, about 5% of RA neurons were inactivated, which would be expected to result in only partial loss of activation of vocal muscles or of coordination with respiratory rhythm, resulting in degradation of syllables controlled by the inactivated neurons. This vocal generation circuit appears to be firmly formed, since silencing of the same group of neurons at different times cause the acoustical alteration of the same song parts.

Bird song singing and learning provide the premier model for learning of sequenced motor generation, as well as neuronal plasticity during the developmental critical period. In

addition to the behavioral analysis of singing and learning processes during development, many physiological, anatomical, and pharmacological techniques have been applied to reveal underlying neuronal mechanisms for this behavior. Although genetically modified songbirds have not been established yet, recent viral vector-based methods have provided new tools for model development (Roberts et al., 2010, Roberts et al., 2012). The present study employed a newly developed pharmacogenetic tool in zebra finches, providing a model that will allow further investigation into generation of motor sequences involved in singing behavior and song learning within the developmental time window.

Acknowledgments

We thank Dr. Hiroshi Takagi for his great technical support for the *in vitro* electrophysiological study, Dr. Elizabeth Ko Mitamura for her technical support for the generation of AAVs and Drs. Aryesh Mukherjee, Mahesh M. Bandi and Colm Connaughton for thoughtful discussions about the mechanics of the avian syrinx. We are also grateful for generous support to Y. Y-S from the Okinawa Institute of Science and Technology Graduate University. This research was partially supported by the Ministry of Education, Culture, Sports, Science, and Technology (MEXT), a Grant-in-Aid for Scientific Research (C) (24500403) to Y. Y-S, a Grant-in-Aid for Scientific Research (B) (24300129) to M.L. and by the MEXT World Premier International Research Center Initiative (WPI) to M.L.

Abbreviations

RA: the robust nucleus of the archistriatum

IVM: ivermectin

CFP: Cyan florescent protein

YFP: Yellow florescent protein

References

Agate R.J., Scott B.B., Haripal B., Lois C. and Nottebohm F. (2009). Transgenic songbirds offer an opportunity to develop a genetic model for vocal learning. Proc Natl Acad Sci USA**106**, 17963-17967.

Amador, A., Perl, Y.S., Mindlin, G.B., and Margoliash, D. (2013). Elemental gesture dynamics are encoded by song premotor cortical neurons. Nature, **495**, 59-64

Ashmore R.C., Bourjaily M., and Schmidt M.F. (2008). Hemispheric coordination is necessary for song production in adult birds. J. Neurophysiol., **99**, 373-385:

Boyden, E.S., Zhang, F., Bamberg, E., Nagel, G., and Deisseroth, K. (2005). Millisecond-timescale, genetically targeted optical control of neural activity. Nat

Neurosci **8**, 1263–1268.

Charlesworth, J.D, Warren, T.L., and Brainard, M.S. (2012). Covert skill learning in a cortical-basal ganglia circuit. Nature **486**, 251–255

Chi, Z., and Margoliash, D. (2001). Temporal precision and temporal drift in brain and behavior of zebra finch song. Neuron **32**, 899 –910.

Fee, M.S., Kozhevnikov, A.A., and Hahnloser, R.H.R. (2004). Neural mechanisms of vocal sequence generation in the songbird. Ann. NY Acad. Sci.**1016**, 153–170.

Fee, M.S., and Leonardo, A. (2001). Miniature motorized microdrive and commutator system for chronic neural recordings in small animals. J. Neurosci. Methods **112**, 83–94.

Fee, M.S., Shraiman, B., Pesaran, B., and Mitra, P.P. (1998). The role of nonlinear dynamics of the syrinx in the vocalizations of a songbird. Nature **395**, 67–71.

Gardner, T., Cecchi, G., Magnasco, M., Laje, R., and Mindlin, G.B. (2001). Simple gestures for birdsongs. Phys. Rev. Letts. **87**, 208101.

Greenewalt, C.H. (1968). Bird song: acoustics and physiology. Washington, DC: Smithsonian Institution.

Gurney, M.E. (1981) Hormonal control of cell form and number in the zebra finch song system. J Neurosci. **1**, 658–673.

Hahnloser, R.H.R., Kozhevnikov, A.A., and Fee, M.S. (2002). An ultra-sparse code underlies the generation of neural sequences in a songbird. Nature **419**, 65–70.

Leonardo, A., and Fee, M.S. (2005). Ensemble coding of vocal control in Bbirdsong. J. Neurosci. **25**, 652-661.

Lerchner, W., Xiao, C., Slimko, E.M., Van Trigt, L., Lester, H. A., and Anderson, D.J. (2007). Reversible silencing of neuronal excitability in behaving mice by a genetically targeted, ivermectin-gated Cl Channel. Neuron **54**, 35-49.

Li, X., Slimko, E.M., and Lester, H.A. (2002). Selective elimination of glutamate activation and introduction of fluorescent proteins into a Caenorhabditis elegans chloride channel. FEBS Lett. **528**, 77–82.

Li, X., Gutierrez D.V., Hanson, M.G., Han, J., Mark, M.D., Chiel, H., Hegemann, P., and Landmesser, L.T. (2005). Fast noninvasive activation and inhibition of neural and network activity by vertebrate rhodopsin and green algae channel rhodopsin. Proc Natl Acad Sci USA **102**, 17816‑1782.

Long, M.A., and Fee, M.S. (2010). Support for a synaptic chain model of neuronal sequence generation. Nature **468**, 394-399

Long, M.A., and Fee, M.S. (2008). Using temperature to analyse temporal dynamics in the songbird motor pathway. Nature **456**, 189-194

McCasland, J., and Konishi, M. (1981). Interaction between auditory and motor activities in an avian song control nucleus. Proc. Natl. Acad. Sci. USA **78**, 7815-7819.

Mindlin, G.B., Gardner, T.J., Goller, F., and Suthers, R. (2003). Experimental support for a

model of birdsong production. Physical Rev. E. Stat. Nonlin. Soft. Matter. Phys. **68**, 041908.

Mooney, R. (2000). Different subthreshold mechanisms underlie song selectivity in identified HVc neurons of the zebra finch. J. Neurosci. **201**, 5420–5436.

Nagel, G., Brauner, M., Liewald, J.F., Adeishvili, N., Bamberg, E. and Gottschalk, A. (2005). Light activation of channel rhodopsin-2 in excitable cells of Caenorhabditis elegans triggers rapid behavioral responses. Curr Biol **15**, 2279–2284.

Nottebohm, F., Kelley, D.B., and Paton, J.A. (1982). Connections of vocal control nuclei in the canary telencephalon. J Comp Neurol **207**, 344 –357.

Olveczky, B.P., Andalman, A.S., Fee, M.S. (2005). Vocal experimentation in the juvenile songbird requires a basal ganglia circuit. PLoS Biol **3** e153

Roberts, T.F., Gobes, S.M., Murugan, M., Ölveczky, B.P., and Mooney, R. (2012). Motor circuits are required to encode a sensory model for imitative learning. Nat. Neurosci. **10**, 1454-1459.

Roberts, T.F., Tschida, K.A., Klein, M.E., and Mooney, R. (2010). Rapid spine stabilization and synaptic enhancement at the onset of behavioural learning. Nature **463**, 948-952.

Slimko, E.M., McKinney, S., Anderson, D.J., Davidson, N., and Lester, H.A. (2002). Selective electrical silencing of mammalian neurons in vitro by the use of invertebrate ligand-gated chloride channels. J. Neurosci. **22**, 7373–7379.

Slimko, E.M., and Lester, H.A. (2003). Codon optimization of Caenorhabditis elegans GluCl ion channel genes for mammalian cells dramatically improves expression levels. J. Neurosci. Methods **124**, 75–81.

Vicario, D.S. (1991). Organization of the zebra finch song control system. II. Functional organization of outputs from nucleus Robustus archistriatalis. J. Comp. Neurol. **309**, 486–494.

Vicario, D.S., and Nottebohm, F. (1988) Organization of the zebra finch song control system: I. Representation of syringeal muscles in the hypoglossal nucleus. J. Comp. Neurol. **271**, 346–354.

Wild, J.M. (1993). Descending projections of the songbird nucleus Robustus archistriatalis. J Comp. Neurol. **338**, 225–241.

Yu, A.C., and Margoliash, D. (1996). Temporal hierarchical control of singing in birds. Science **273**, 1871–1875.

Figure legends

Figure 1

A: Construction of adeno-associated viral (AAV) vectors to express either subunit (α or β) of IVM-gated chloride channels (optGluCl) from *Caenorhabditis elegans*. **B**: Virus was injected

into the zebra finch forebrain premotor area, robust nucleus of the Arcopallium (RA). Expression of tagged florescent proteins CFP and YFP could be detected after more than two weeks. In most cases, expression of both CFP and YFP was detected.

Figure 2

Suppression of neuronal activity with invermectin application to acute slices. **A:** Histological verification of a recorded neuron (arrow head) with expression of CFP and YFP in confocal images. The recorded cell was labeled with Alexa647 delivered through the recording electrode (right) and expressed both CFP (left) and YFP (middle). **B:** Sample trace of activity from an RA neuron that expressed both CFP and YFP, voltage clamped at 0 mV before and during invermectin (IVM) bath application, and 15 min after washing. **C**: Firing rate measured as action-potential currents during time progression (5 events each) from before, during, 15 min after, and 25 min after IVM application), and normalized with the rate before IVM application, recorded in CFP- and YFP-positive neurons (left) and CFP and YFP-negative neurons (right). Each symbol denotes recording from different neurons (4 neurons each for CFP/YFP positive and negative).

Figure 3

Systemic injection of IVM decreased spontaneous spiking activity of an RA neuron recorded

in an anesthetized, virus-infected bird. **A.** Firing rate of RA spontaneous activity. After systemic injection of IVM (1.25mg / kg BW), the firing the rate decreased. **B.** Representative traces of extracellular RA neuronal spiking activity before (top) and after (bottom) IVM injection. **C.** Interspike-interval (ISI) histogram of RA spontaneous activity measured during 10 min periods before and after IVM injection (shown as an open rectangle in A).

Figure 4

Effects of suppression of RA neuronal activity by IVM injection on singing behavior.

A: Timeline of experimental procedures. IVM (1.25 mg/kg BW) was test-injected before virus injection to check innate sensitivity to IVM and to establish a baseline effect on singing behavior. Then AAVGluClα and AAVGluClβ were injected into RA with stereotaxic coordination. More than 2 weeks later, which was sufficient for full expression of α and β subunits of the GluCl channel in a group of RA neurons, IVM was injected again to determine the effect of suppression of RA neuronal activity. A third injection of IVM was made 3 weeks thereafter to confirm the effect of silencing of RA neuronal activities. **B:** Zebra finch songs were transiently degraded by inactivation of a subset of RA neurons, but not when only IVM was applied. Song similarity at each time point, normalized to the birds' own template songs, which were recorded just before the test and IVM injection day, was

determined. Whereas IVM injection did not affect song similarity before virus injection, it decreased song similarity to the template significantly after expression of GluCl channels via the viral infection. The same effect could be repeated by the second injection of IVM after recovery. Each symbol denotes similarity of different birds (n=7). **C:** Average number of syllables in a motif of songs during the time course of IVM injection in 5 birds with degraded songs after IVM injection. **D**: Average number of identified syllables matching the sypical template in song motifs during the course of IVM action in 5 birds with degraded songs after IVM injection. Each symbol denotes data from a specific bird. Symbols in **B, C** and **D** denote data from the same birds. Note that some birds did not change the number of syllables, but decreased the number of identifiable syllables (degraded). Others decreased the number of syllables in a motif (stopped in the middle or dropped syllables).

Figure 5

Representative confocal images of RA neuronal expression of CFP, YFP and immunohistological staining for GFP and NeuN.

Figure 6

Effects of suppression of RA neuronal activity by IVM injection in the singing behavior of bird Yellow050. **A**: Spectrograms of songs of the same bird before, 1 and 12 days after

IVM injection following virus injection. Note that acoustic structure of syllable #2 degraded, and repetition of syllable #3 and #4 occurs more frequently one day after IVM injection. **B**: Number of each type of syllable that matched the typical syllable template within 30 motifs of songs before, and 1 and 12 days after the second IVM injection. **C:** Average duration of each syllable identified by visual inspection before and 1 day after IVM injection. Duration of syllables #3 and #4 were slightly, but significantly decreased following IVM injection ($p<0.05$, unpaired t-test). Durations of other syllables did not change. **D:** Average intervals between syllables identified by visual inspection (beginning of a syllable to the beginning of the next syllable) before and 1 day after IVM injection. Intervals between syllables #2-3 and syllables #3-4 were slightly, but significantly increased following IVM injection ($p<0.05$, unpaired t-test), while the interval between syllables #1-2 did not change. **E**: Average gaps between syllables identified with visual inspection (silent period between syllables) before and 1 day after IVM injection. Gaps between syllables #2-3 and syllables #3-4 were significantly increased following IVM injection ($p<0.05$, unpaired t-test), while gap between syllables #1-2 did not change.

Figure 7

Effects of suppression of RA neuronal activity by IVM injection in the singing behavior of bird Orange058. **A**: Spectrograms of songs of the same bird before, 3 hrs and 1 day after

IVM injection following virus injection. Note that acoustic structure of syllable #3 degraded, while syllable #2 changed little. **B**: Number of each type of syllable that matched the typical syllable template in 30 song motifs before, 3 hrs and 1 day after the first IVM injection. **C:** Average duration of each syllable identified by visual inspection before and 3hrs day after IVM injection. Duration of all syllable were slightly, but significantly increased following IVM injection ($p<0.05$, unpaired t-test). **D:** Average intervals between syllables identified by visual inspection (beginning of a syllable to the beginning of the next syllable) before and 3hrs after IVM injection. The interval between syllables #2-3 was slightly, but significantly increased following IVM injection ($p<0.05$, unpaired t-test), while the interval between syllables #1-2 did not change. **E**: Average gaps between syllables identified by visual inspection (silent period between syllables) before and 3 hrs after IVM injection. The gap between syllables #1-2 was slightly, but significantly decreased following IVM injection ($p<0.05$, unpaired t-test), while the gap between syllables #2-3 did not change.

Figure 8

Effects of suppression of RA neuronal activity by IVM injection in the singing behavior of bird Orange064. **A**: Spectrograms of songs of the same bird before, 2, and 4 days after IVM injection following virus injection. Note that songs stopped at syllable #4 after the IVM

injection. **B**: Number of each type of syllable that matched the typical syllable template within 30 song motifs before, 2, and 4 days after the first IVM injection. Durations of other syllables did not change. **C:** Average duration of each syllable identified by visual inspection before and 2 days after IVM injection. Duration of syllables #2, #3, and #4 were slightly, but significantly decreased, while the duration of syllable #1 increased following IVM injection ($p<0.05$, unpaired t-test). **D:** Average intervals between syllables identified by visual inspection (beginning of a syllable to the beginning of the next syllable) before and 2 days after IVM injection. Intervals between syllables #1-2 and syllables #2-3 were slightly, but significantly increased following IVM injection ($p<0.05$, unpaired t-test), while interval between syllables #3-4 decreased ($p<0.05$, unpaired t-test). **E**: Average gaps between syllables identified by visual inspection (silent period between syllables) before and 2 days after IVM injection. The gap between syllables #2-3 was increased following IVM injection ($p<0.05$, unpaired t-test), while the gap between other syllables did not change.

Figure 9

Effects of suppression of RA neuronal activity by IVM injection in the singing behavior of bird Green001. **A**: Spectrograms of songs of the same bird before, 5, and 8 day after IVM injection following virus injection. Note that songs stopped at syllable #2 or #3 with degraded acoustic structure after the IVM injection. **B**: Number of each type of syllable that

matched the typical syllable template within 30 song motifs before, 5, and 8 days after the first IVM injection. **C:** Average duration of each syllable identified with visual inspection before and 5 days after IVM injection. Duration of syllables #1 and #2 were significantly decreased ($p<0.05$, unpaired t-test). There is no syllable #5 detected by visual inspection. **D:** Average intervals between syllables identified with visual inspection (beginning of a syllable to the beginning of the next syllable) before and 5 days after IVM injection. Intervals between syllables #1-2 were slightly, but significantly decreased while intervals between syllables #3-4 increased following IVM injection ($p<0.05$, unpaired t-test). Intervals between syllables #2-3 did not change after the IVM injection. Intervals between syllables #4-5 could not be measured as there was no syllable 5 detected. **E**: Average gaps between syllables identified by visual inspection (silent period between syllables) before and 5 days after IVM injection. The gap between syllables 2-3 was significantly increased following IVM injection ($p<0.05$, unpaired t-test), while the gap between other syllables did not change. Gaps between syllables 4-5 could not be measured as there was no syllable 5 detected.

Figure 10

Effects of suppression of RA neuronal activity by IVM injection in the singing behavior of bird Orange060. **A**: Spectrograms of songs of the same bird before, 1 and 3 day after IVM

injection following virus injection. Note that there is no syllable 4 after the IVM injection. **B**: Number of each type of syllable that matched the typical syllable template within 30 motifs of songs before, 1 and 3 days after the first IVM injection. No syllable 4 was identified 1 day after injection, and the number of syllables #2 and #3 had not changed at that time. **C:** Average duration of each syllable identified by visual inspection before and 1 day after IVM injection. Duration of syllables did not change. **D:** Average intervals between syllables identified by visual inspection (beginning of a syllable to the beginning of the next syllable) before and 1 day after IVM injection. Intervals between syllables #3-4 or syllables #4-5 could not be measured, as there was no syllable 4. Intervals between syllables #2-3 were slightly, but significantly increased following IVM injection ($p<0.05$, unpaired t-test), while intervals between other syllables did not change after IVM injection. **E**: Average gaps between syllables identified with visual inspection (silent period between syllables) before and 1 day after IVM injection. Gaps between syllables did not change.

Figure 11

Durations of whole song motifs before and after IVM injections in the bird that changed the song with suppression of RA neuronal activity. Duration of whole song motif slightly, but significantly increased in all birds, except bird Green001, in which duration of song motifs decreased significantly ($p<0.05$, unpaired t-test). As birds Orange064 and Green001

stopped their songs in the middle of song motifs after IVM injection, duration of the remaining parts were measured and compared.

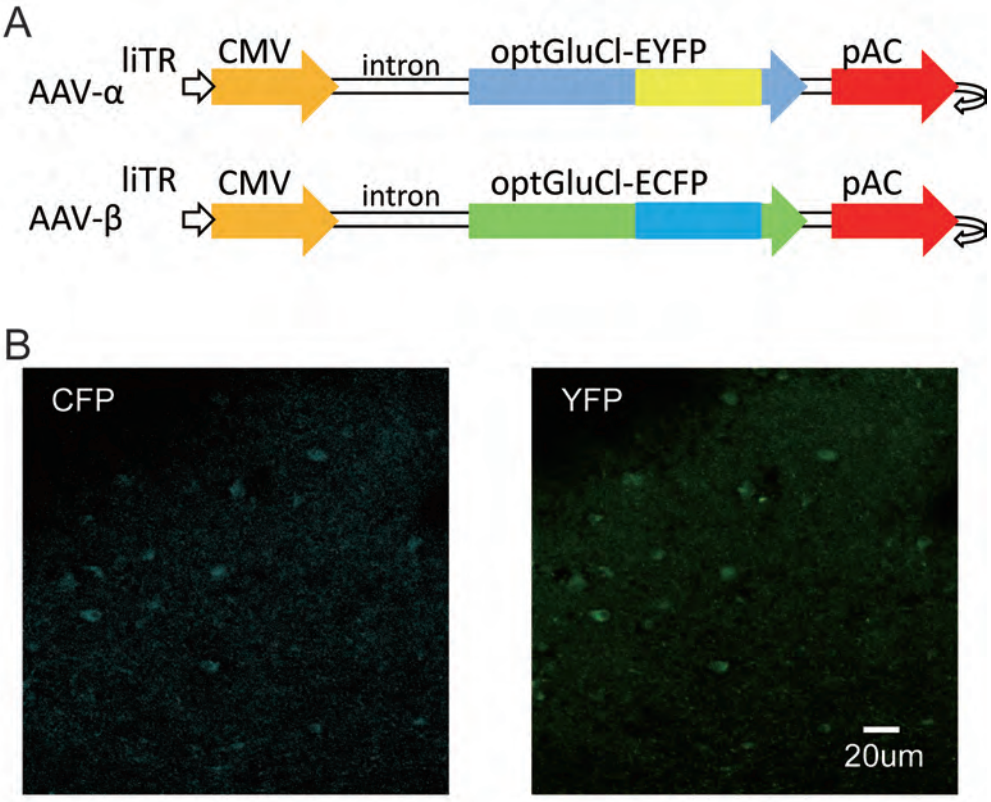
A
AAV-α
liTR
CMV
intron
optGluCl-EYFP
pAC
AAV-β
liTR
CMV
intron
optGluCl-ECFP
pAC
B
CFP
YFP
20um

Figure 1

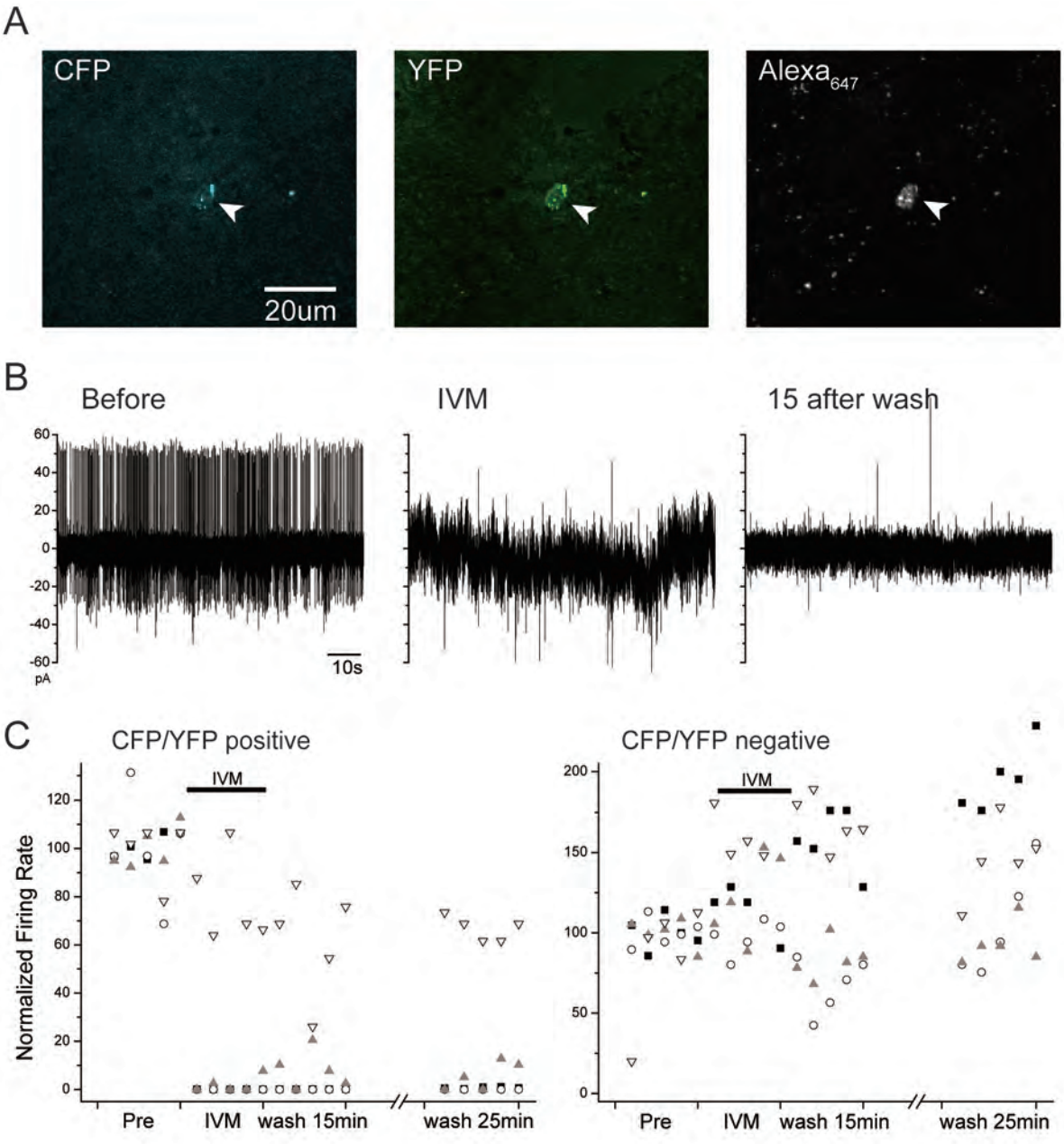
A
CFP
YFP
Alexa647
20um
B
Before
IVM
15 after wash
60
40
20
0
-20
-40
-60
pA
10s
C
CFP/YFP positive
CFP/YFP negative
IVM
Normalized Firing Rate
120
100
80
60
40
20
0
200
150
100
50
Pre
IVM
wash 15min
wash 25min

Figure 2

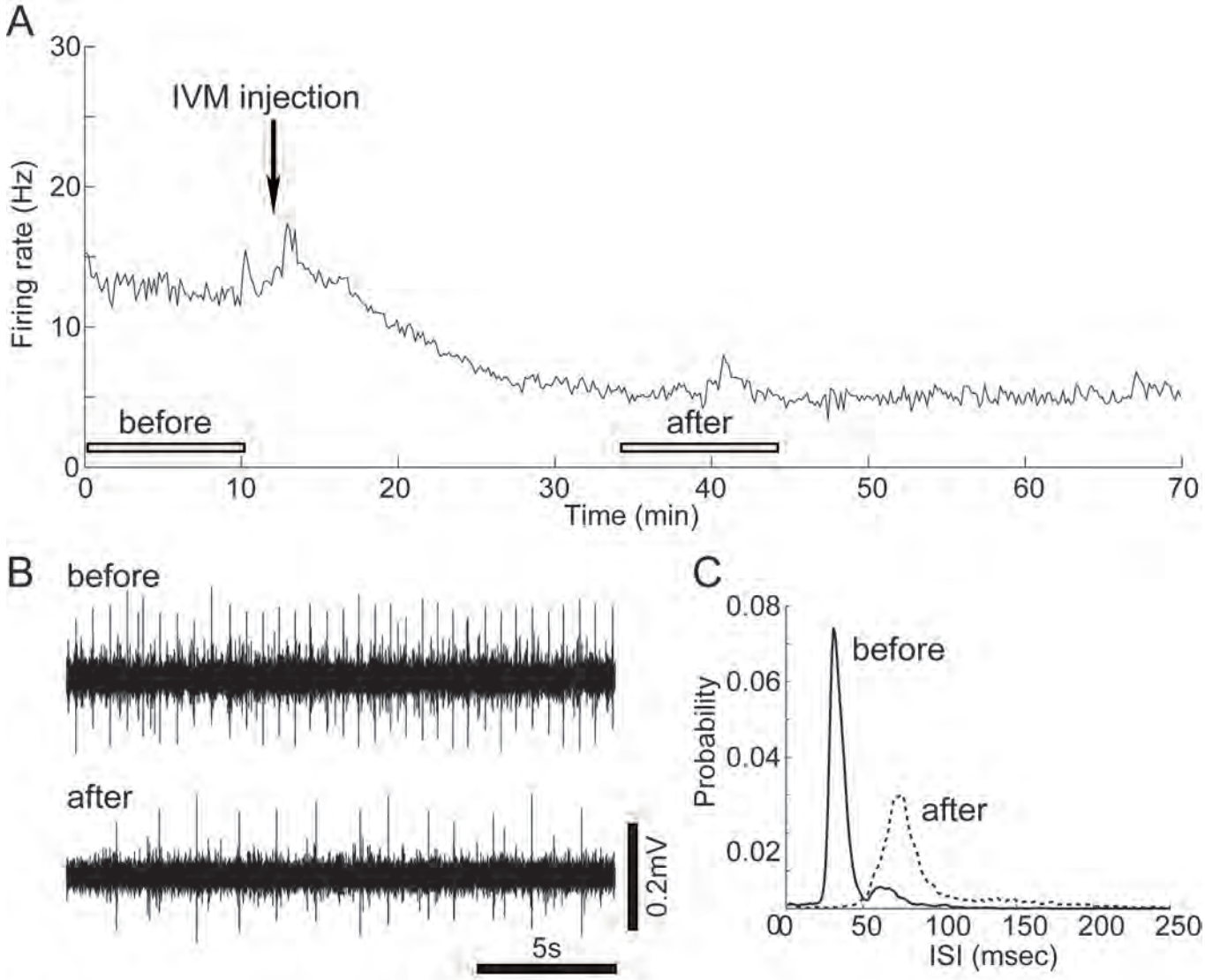
A
30
20
10
0
Firing rate (Hz)
IVM injection
before
after
0
10
20
30
40
50
60
70
Time (min)
B
before
after
0.2mV
5s
C
0.08
0.06
0.04
0.02
Probability
before
after
00
50
100
150
200
250
ISI (msec)

Figure 3

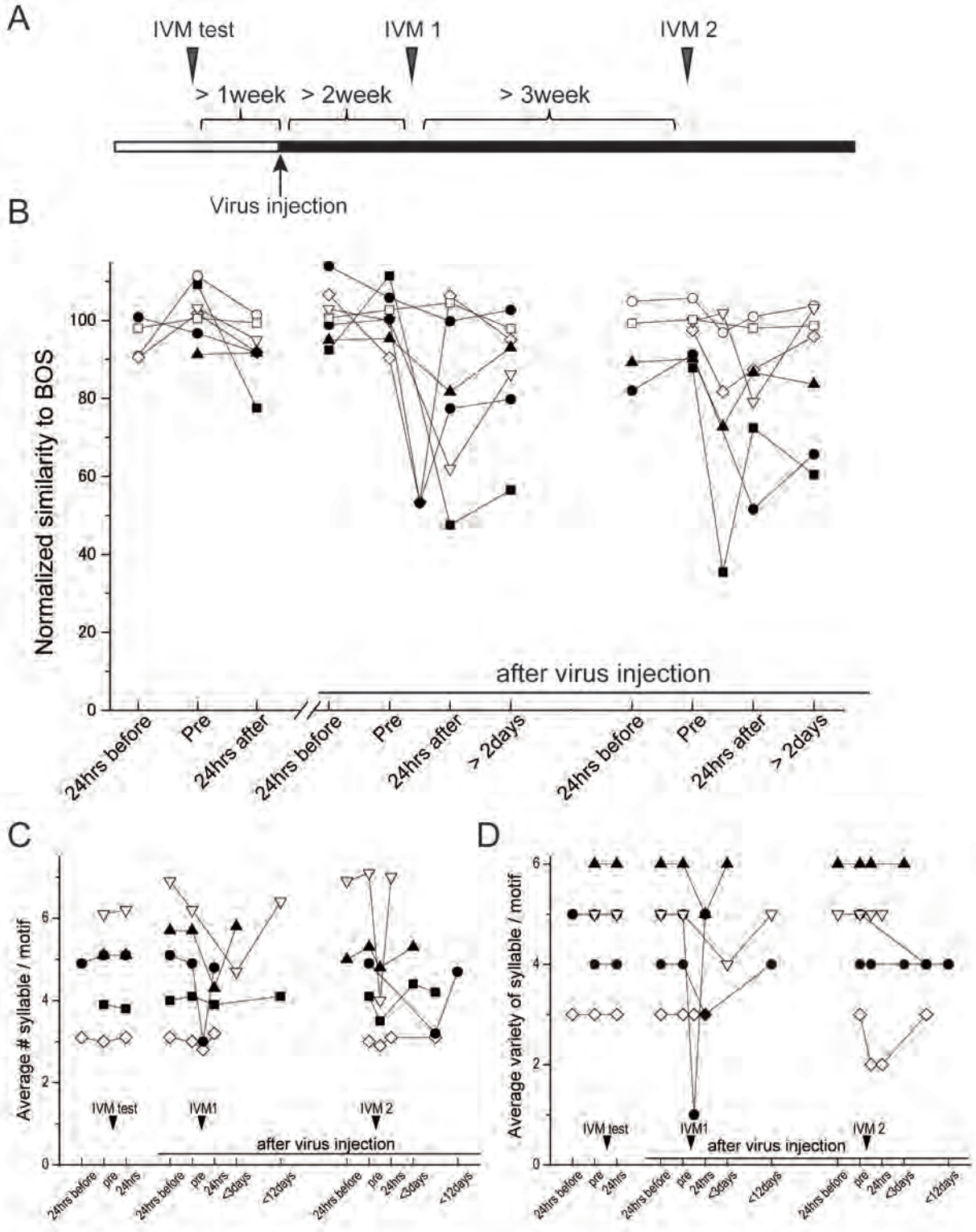
A
IVM test
IVM 1
IVM 2
> 1week
> 2week
> 3week
Virus injection
B
Normalized similarity to BOS
100
80
60
40
20
0
after virus injection
24hrs before
Pre
24hrs after
24hrs before
Pre
24hrs after
> 2days
24hrs before
Pre
24hrs after
> 2days
C
Average # syllable / motif
6
4
2
0
IVM test
IVM1
IVM 2
after virus injection
24hrs before
pre
24hrs
24hrs before
pre
24hrs
<3days
<12days
24hrs before
pre
24hrs
<3days
<12days
D
Average variety of syllable / motif
6
4
2
0
IVM test
IVM1
IVM 2
after virus injection
24hrs before
pre
24hrs
24hrs before
pre
24hrs
<3days
<12days
24hrs before
pre
24hrs
<3days
<12days

Figure 4

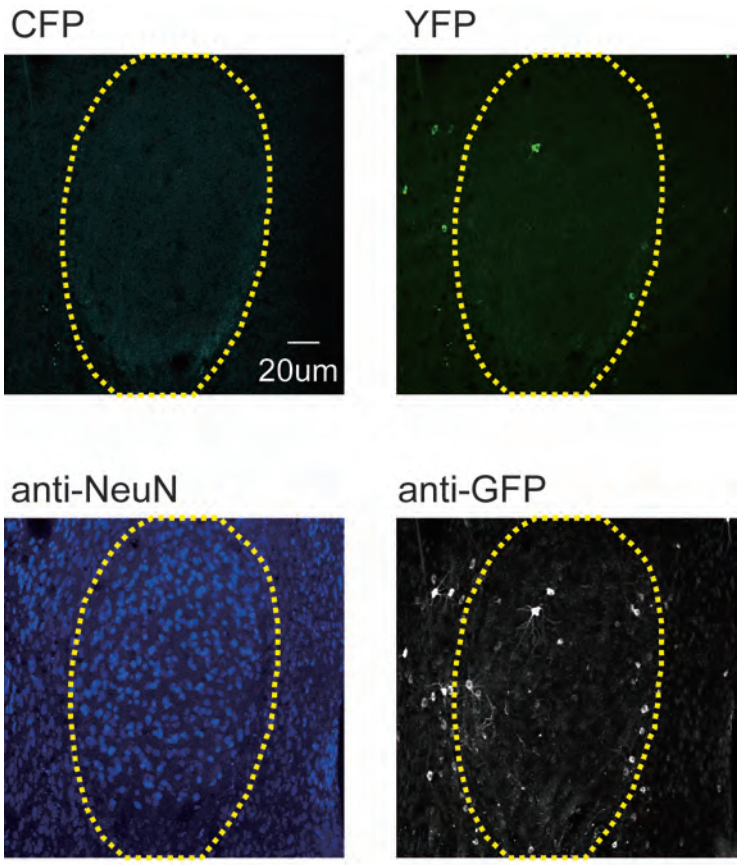

Figure 5

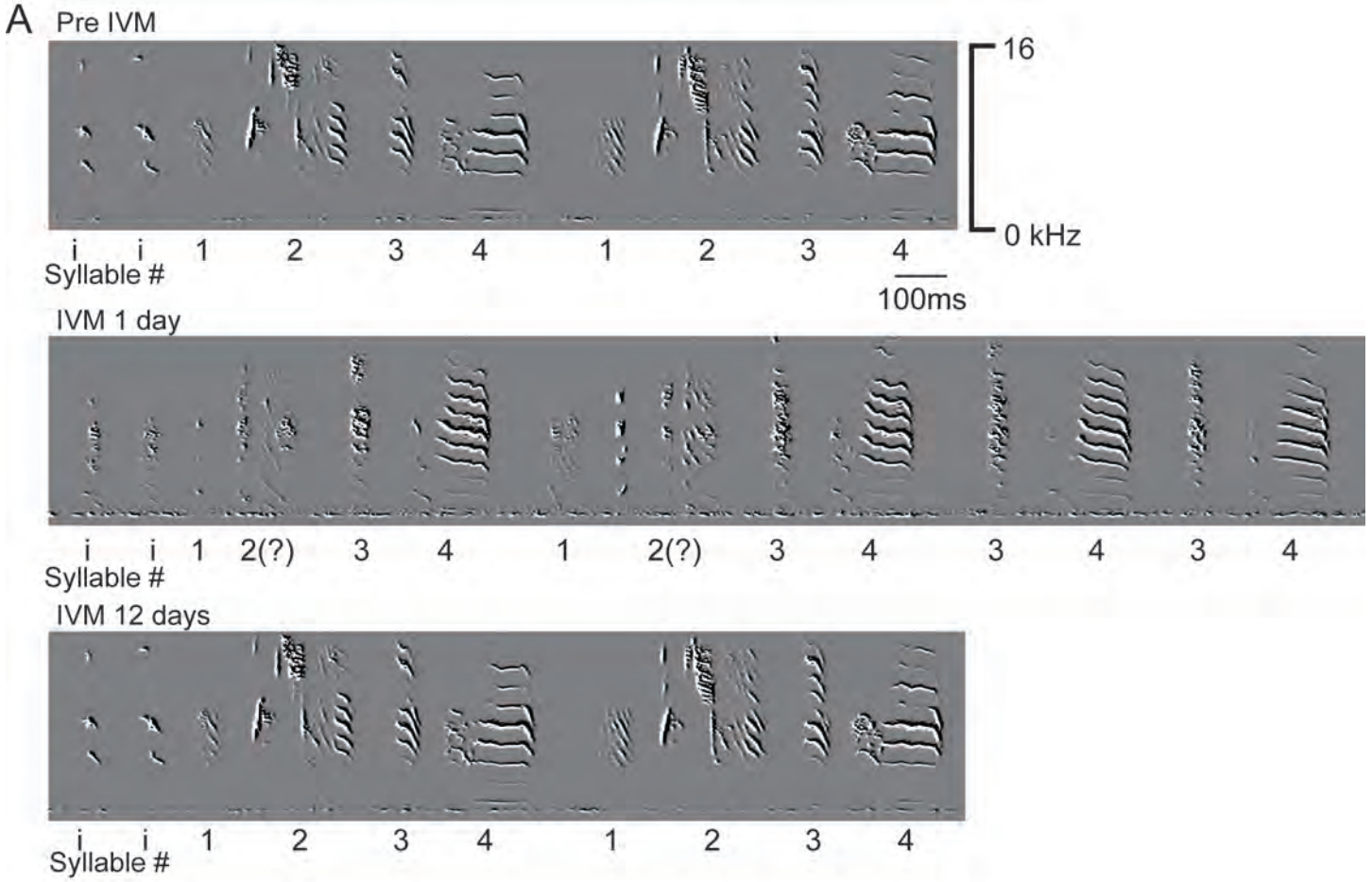
A
Pre IVM
16
0 kHz
i i 1 2 3 4 1 2 3 4
Syllable #
100ms
IVM 1 day
i i 1 2(?) 3 4 1 2(?) 3 4 3 4 3 4
Syllable #
IVM 12 days
i i 1 2 3 4 1 2 3 4
Syllable #

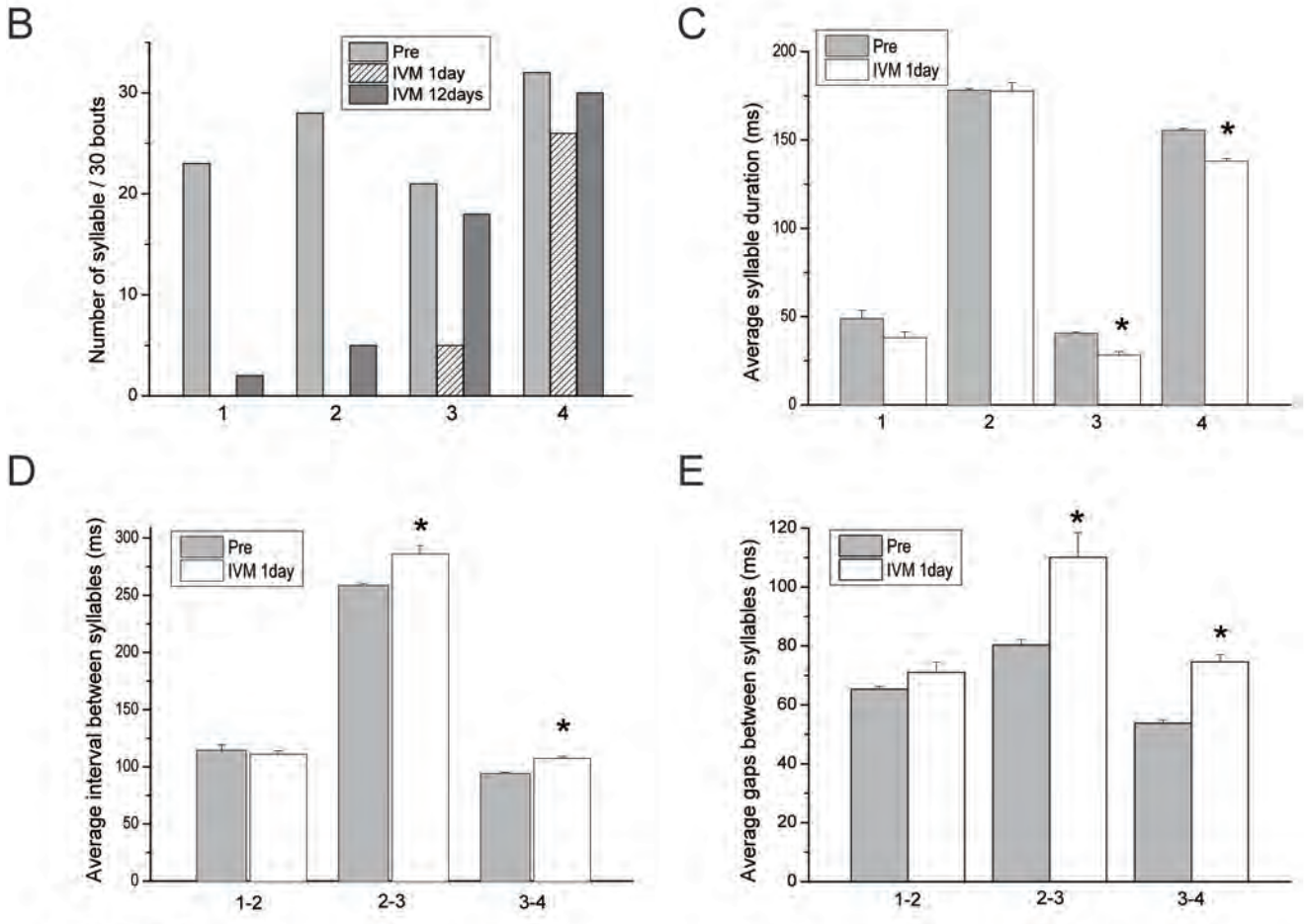
B
Number of syllable / 30 bouts
Pre
IVM 1day
IVM 12days
C
Average syllable duration (ms)
Pre
IVM 1day
D
Average interval between syllables (ms)
Pre
IVM 1day
1-2
2-3
3-4
E
Average gaps between syllables (ms)
Pre
IVM 1day
1-2
2-3
3-4

Figure 6

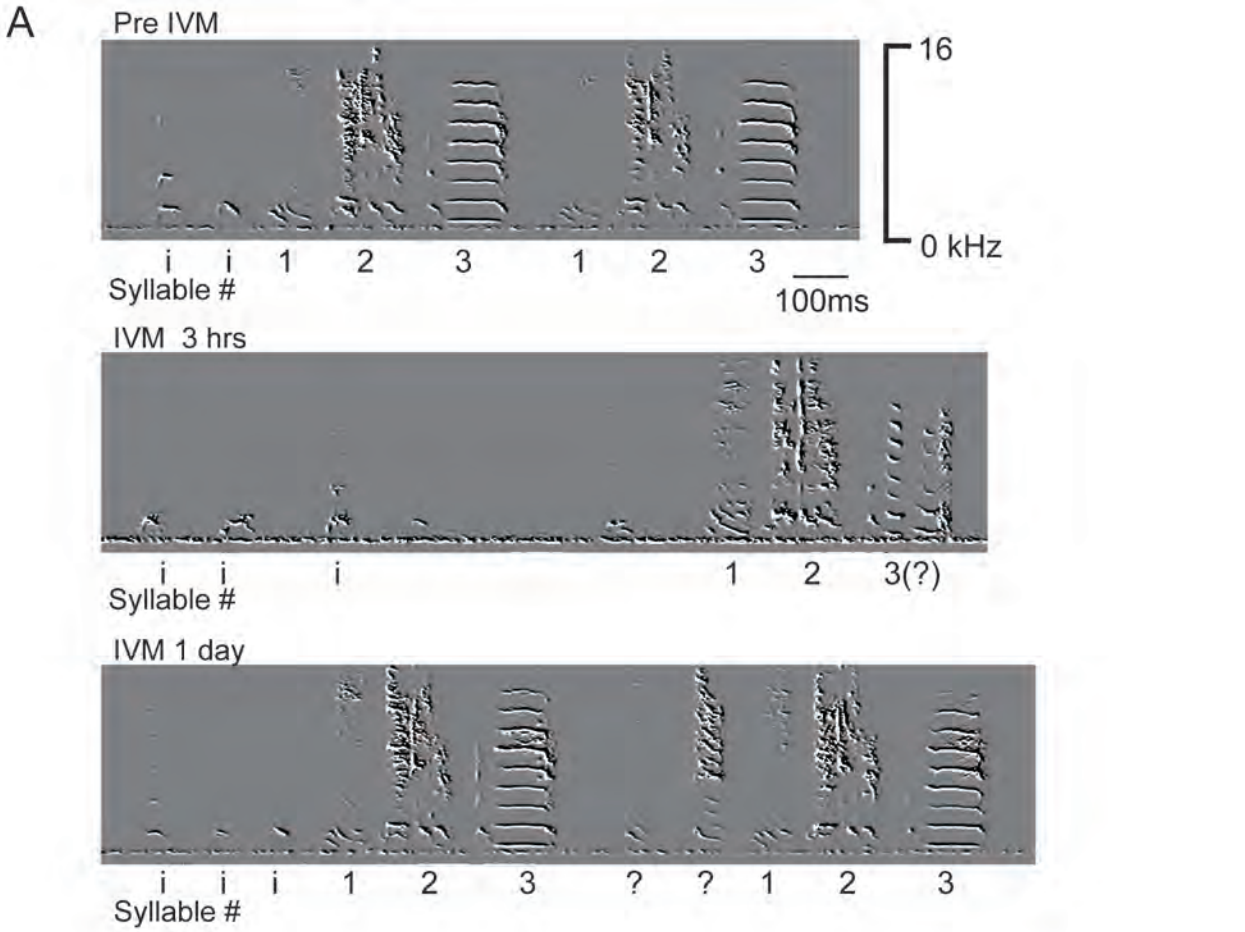
A
Pre IVM
16
0 kHz
i i 1 2 3 1 2 3
Syllable #
100ms
IVM 3 hrs
i i i 1 2 3(?)
Syllable #
IVM 1 day
i i i 1 2 3 ? ? 1 2 3
Syllable #

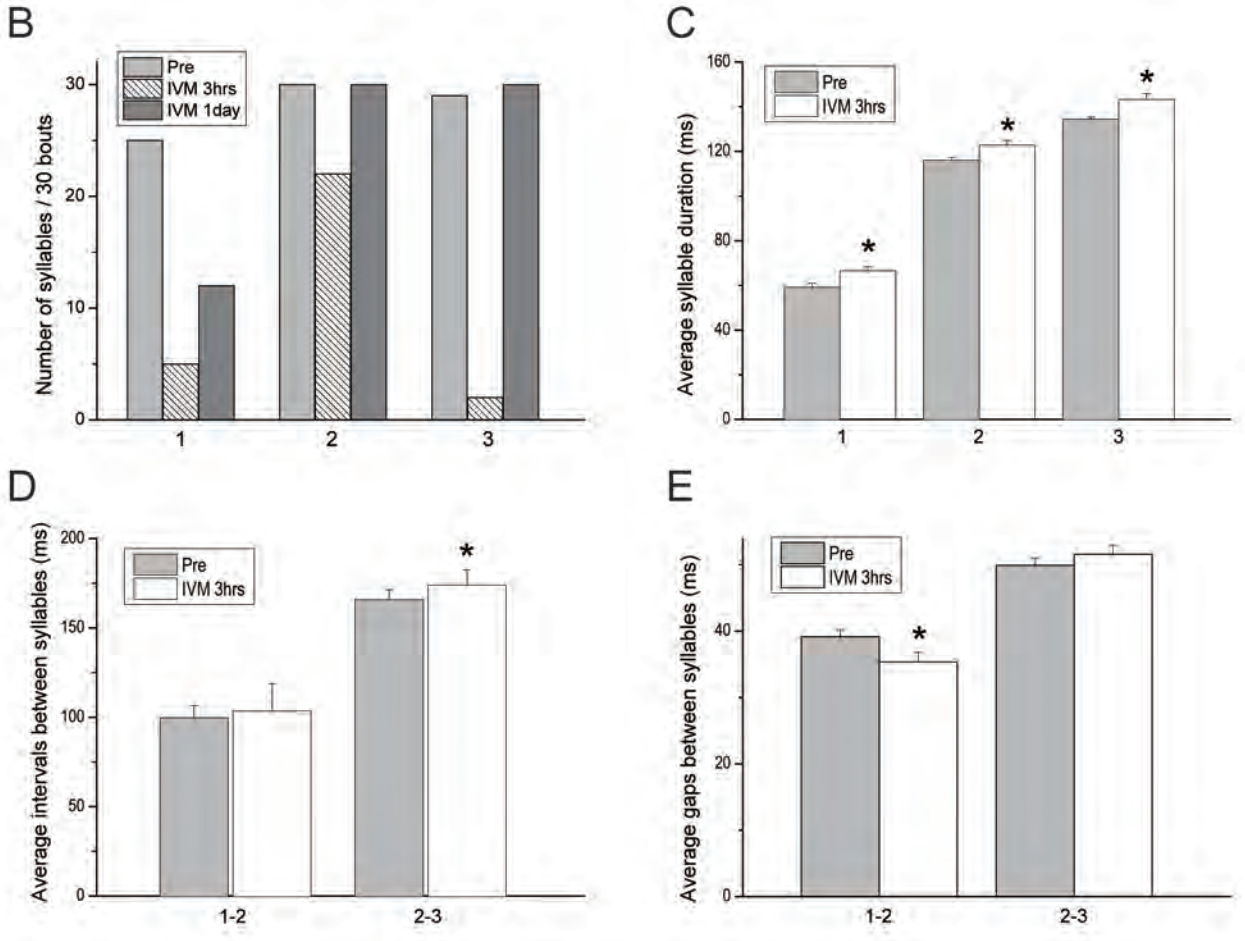
B
Pre
IVM 3hrs
IVM 1day
Number of syllables / 30 bouts
0
10
20
30
1
2
3
C
Pre
IVM 3hrs
Average syllable duration (ms)
0
40
80
120
160
*
*
*
1
2
3
D
Pre
IVM 3hrs
Average intervals between syllables (ms)
0
50
100
150
200
*
1-2
2-3
E
Pre
IVM 3hrs
Average gaps between syllables (ms)
0
20
40
*
1-2
2-3

Figure 7

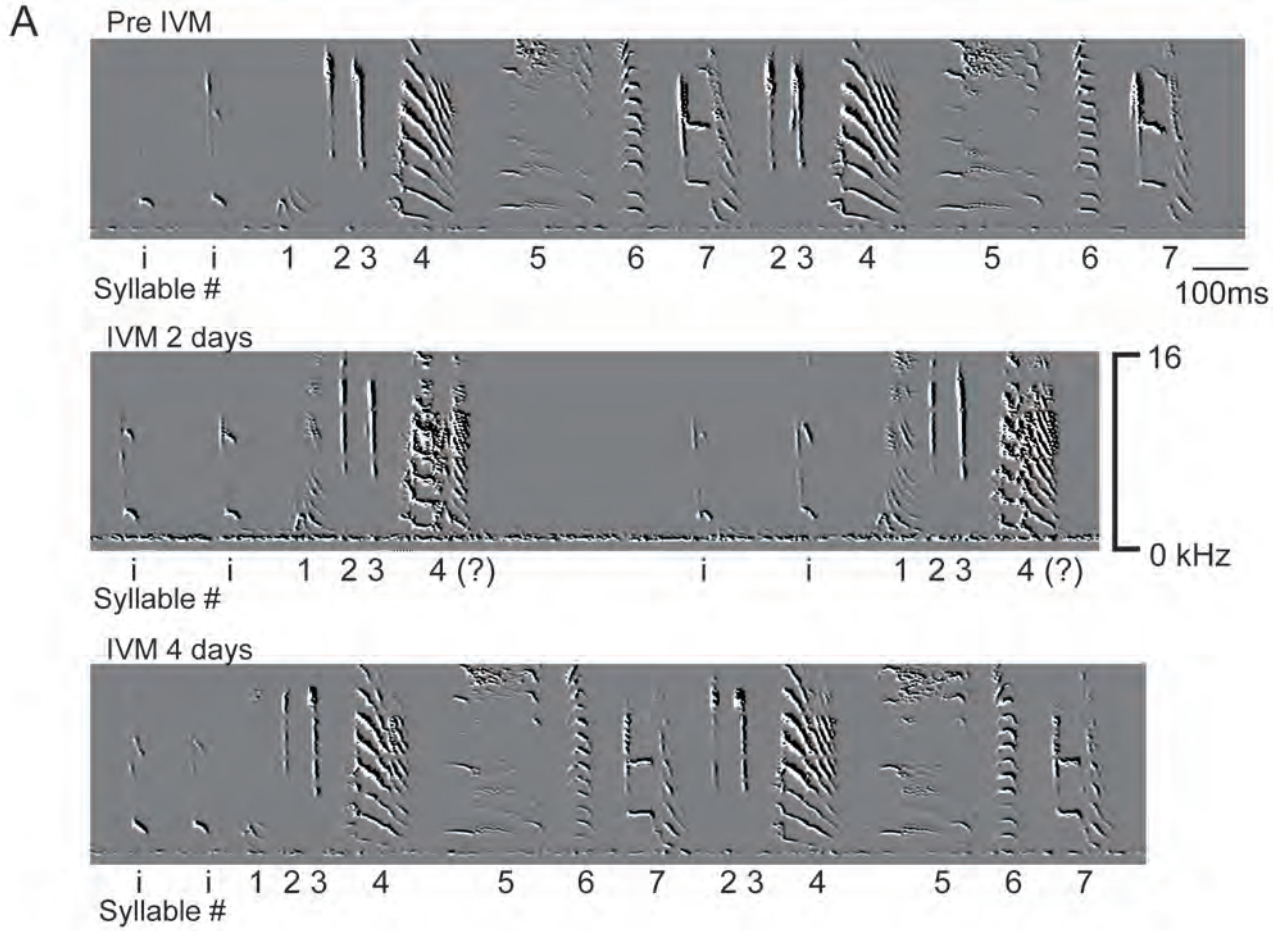
A
Pre IVM
i i 1 2 3 4 5 6 7 2 3 4 5 6 7
Syllable #
100ms
IVM 2 days
16
0 kHz
i i 1 2 3 4 (?) i i 1 2 3 4 (?)
Syllable #
IVM 4 days
i i 1 2 3 4 5 6 7 2 3 4 5 6 7
Syllable #

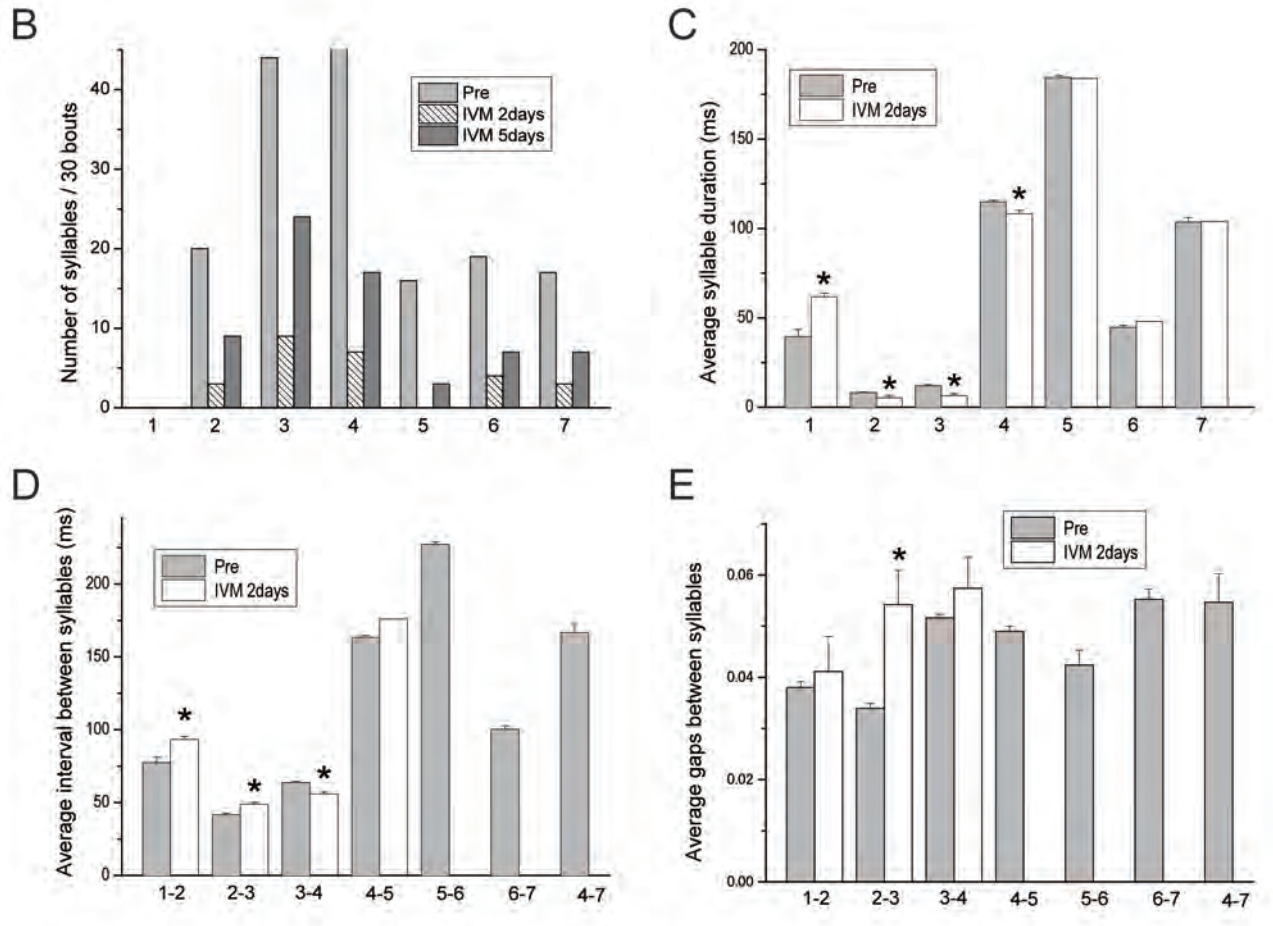
B
Number of syllables / 30 bouts
Pre
IVM 2days
IVM 5days
C
Average syllable duration (ms)
Pre
IVM 2days
D
Average interval between syllables (ms)
Pre
IVM 2days
1-2 2-3 3-4 4-5 5-6 6-7 4-7
E
Average gaps between syllables
Pre
IVM 2days
1-2 2-3 3-4 4-5 5-6 6-7 4-7

Figure 8

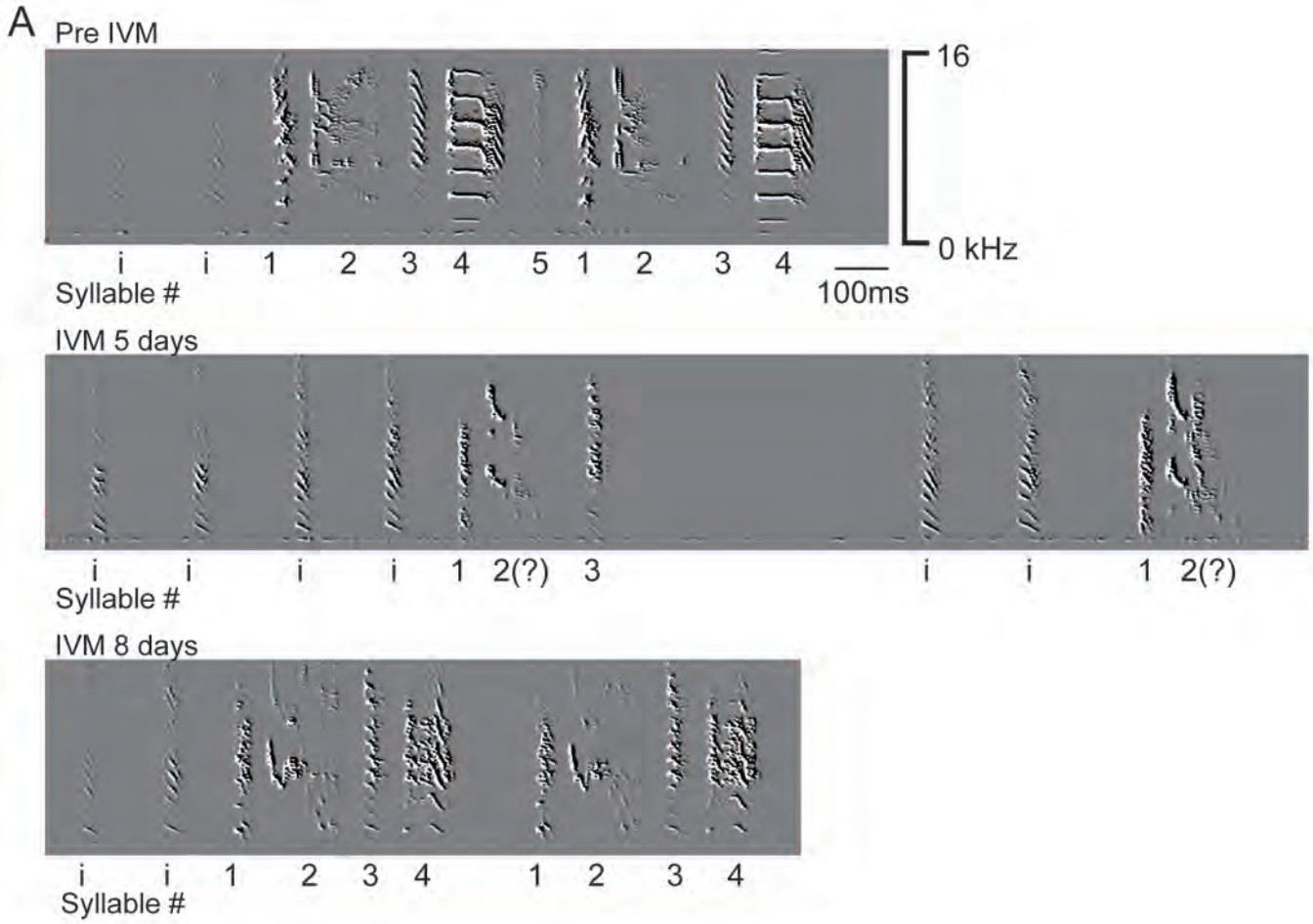
A
Pre IVM
16
0 kHz
i i 1 2 3 4 5 1 2 3 4
Syllable #
100ms
IVM 5 days
i i i i 1 2(?) 3 i i 1 2(?)
Syllable #
IVM 8 days
i i 1 2 3 4 1 2 3 4
Syllable #

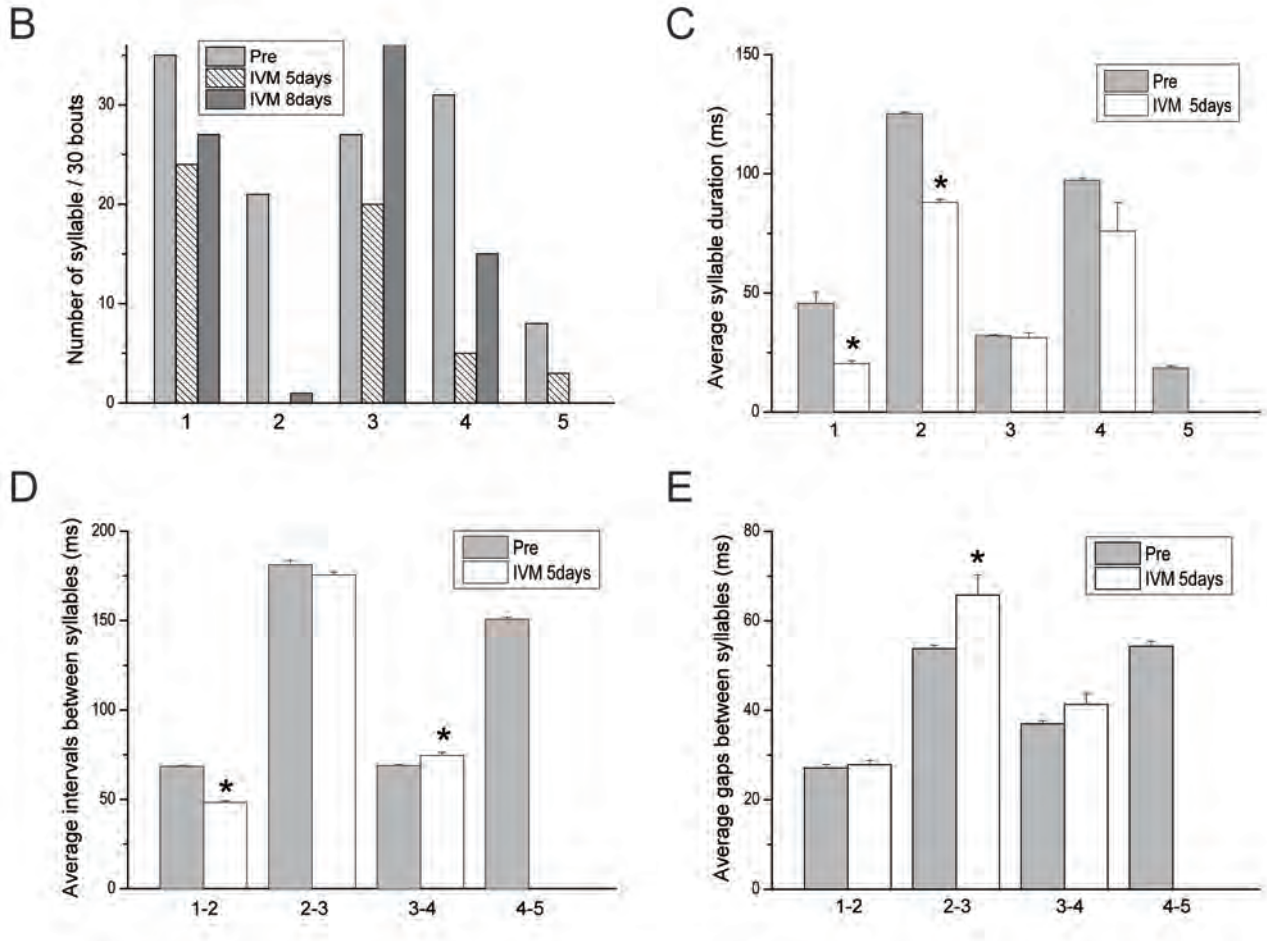
B
Pre
IVM 5days
IVM 8days
Number of syllable / 30 bouts
C
Pre
IVM 5days
Average syllable duration (ms)
D
Pre
IVM 5days
Average intervals between syllables (ms)
1-2
2-3
3-4
4-5
E
Pre
IVM 5days
Average gaps between syllables (ms)

Figure 9

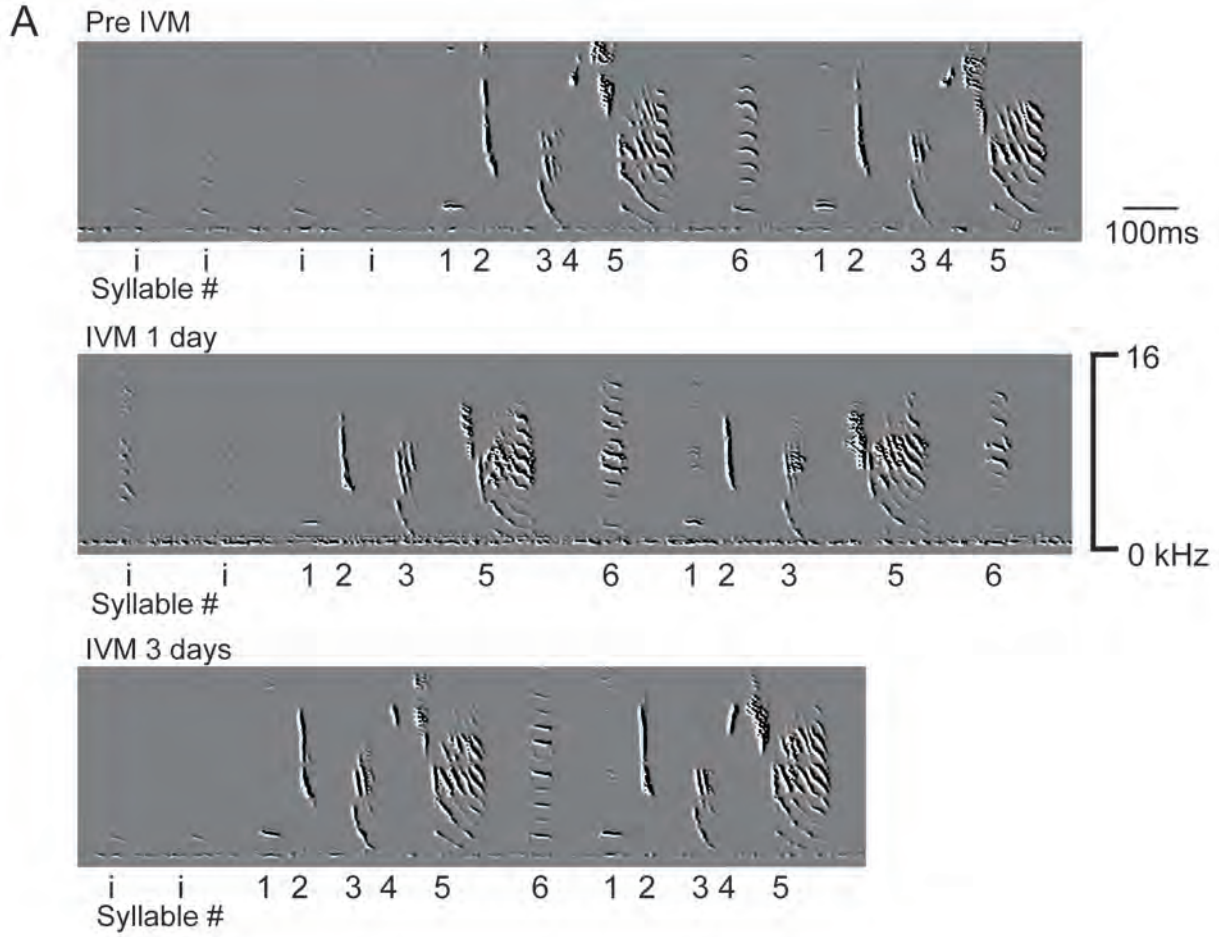
A
Pre IVM
100ms
i i i i 1 2 3 4 5 6 1 2 3 4 5
Syllable #
IVM 1 day
16
0 kHz
i i 1 2 3 5 6 1 2 3 5 6
Syllable #
IVM 3 days
i i 1 2 3 4 5 6 1 2 3 4 5
Syllable #

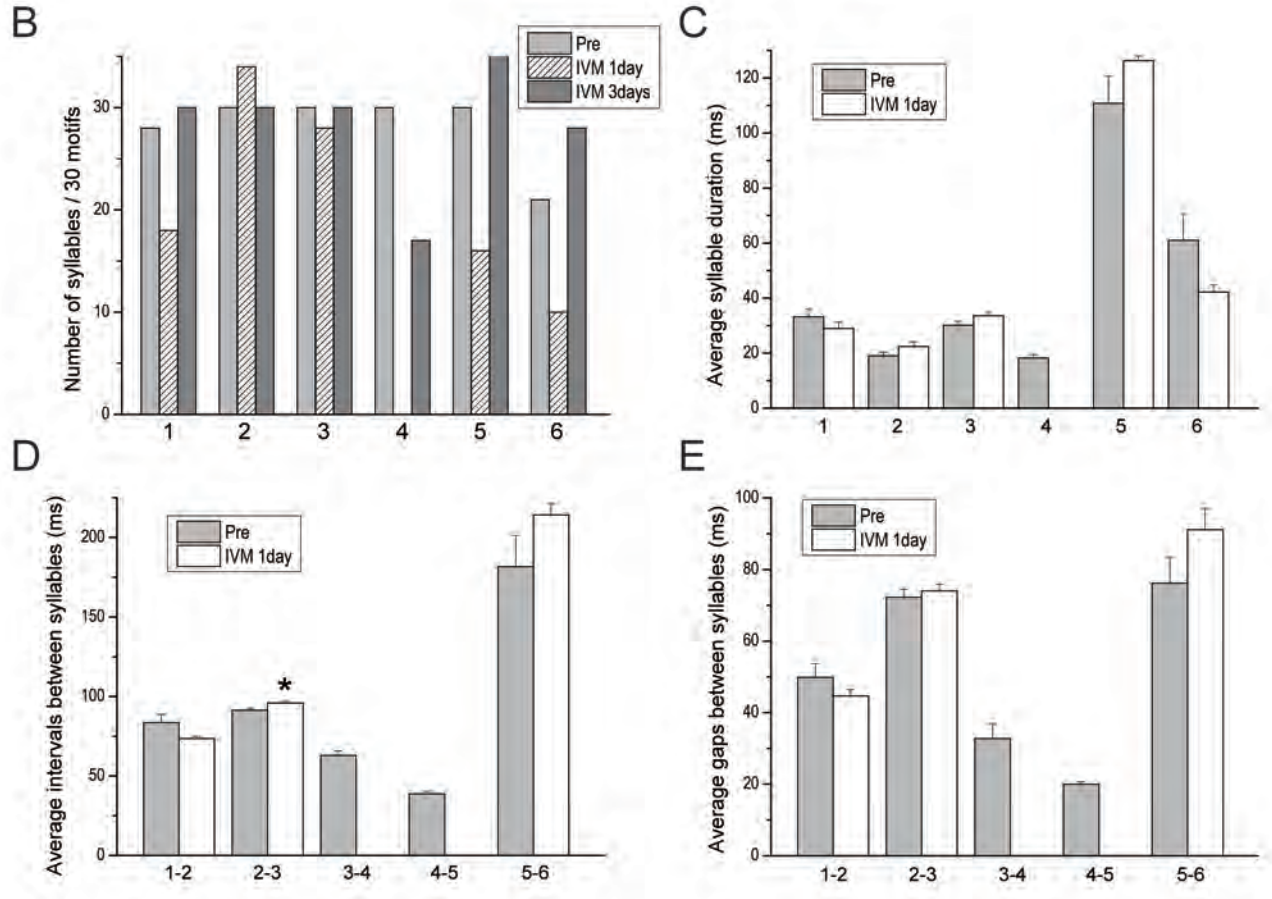
B
Number of syllables / 30 motifs
Pre
IVM 1day
IVM 3days
C
Average syllable duration (ms)
Pre
IVM 1day
D
Average intervals between syllables (ms)
Pre
IVM 1day
*
1-2
2-3
3-4
4-5
5-6
E
Average gaps between syllables (ms)
Pre
IVM 1day
1-2
2-3
3-4
4-5
5-6

Figure 10

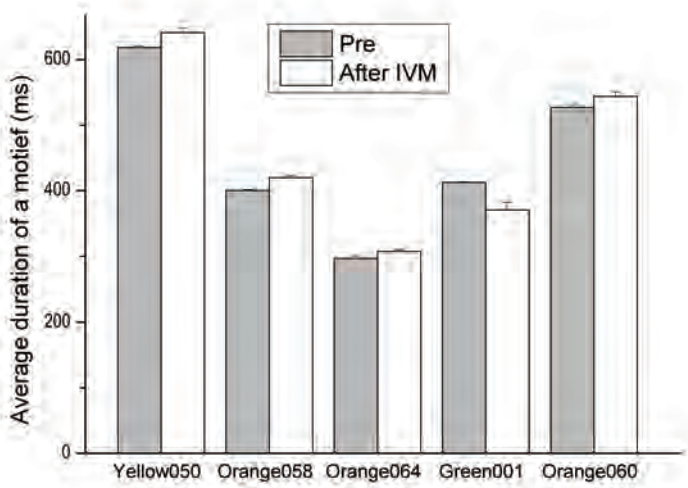
Pre
After IVM
Average duration of a motief (ms)
600
400
200
0
Yellow050
Orange058
Orange064
Green001
Orange060

Figure 11